

Int. J. Electrochem. Sci., 13 (2018) 5589 – 5602, doi: 10.20964/2018.06.39

**International Journal of
ELECTROCHEMICAL
SCIENCE**

www.electrochemsci.org

Electrocatalytical reduction of bromocyclopentane and iodobenzene using Cobalt(III) and Nickel(II) Tris- and Bis-bidentates Schiff Bases Complexes

Ali Ourari^{1,*}, Amina Alouache¹, Djouhra Aggoun^{1,*}, Ramiro Ruiz-Rosas², Emilia Morallon²

¹ Laboratoire d'électrochimie, d'Ingénierie Moléculaire et de Catalyse Rédox (LEIMCR), Faculté de Technologie, Université Sétif-1, Route de Béjaia, 19000, Algeria.

² Departamento de Química Física, Instituto Universitario de Materiales, Universidad de Alicante, Ap.99, 03080 Alicante, Spain

*E-mail: alourari@yahoo.fr, aggoun81@yahoo.fr

Received: 17 February 2018 / *Accepted:* 11 April 2018 / *Published:* 10 May 2018

The following bidentate Schiff base: 2-[(4-Methoxybenzyl)iminomethyl]-phenol (HL), was employed as an asymmetric ligand in the synthesis of two mononuclear nickel(II) and cobalt(III) complexes (Ni(II)-2L and Co(III)-3L). This ligand has been synthesized via condensation of salicylaldehyde and 4-methoxybenzylamine in methanolic solution, while the both complexes result from complexation of metal(II) chloride hydrate salts with HL. These coordination compounds were structurally characterized by elemental analysis, FT-IR, UV-Vis, ¹H NMR and ¹³C NMR spectral studies. Moreover, the electrochemical properties of both complexes were studied by cyclic voltammetry in DMF solution containing 0.1 M tetra-n-butylammonium tetrafluoroborate (Et₄NBF₄). This study reveals that each complex showed successively two redox couples: M(III)/M(II) and M(II)/M(I). Finally, the electrocatalytic activity of these complexes has been examined and it has been found that the both complexes worked as effective homogeneous electrocatalysts for the electroreduction of bromocyclopentane and iodobenzene using glassy carbon as working electrode.

Keywords: Bidentate Schiff base, Bis-bidentate Nickel(II) complex, Tris-bidentate cobalt(III) complex, Cyclic voltammetry, Homogeneous electrocatalysis.

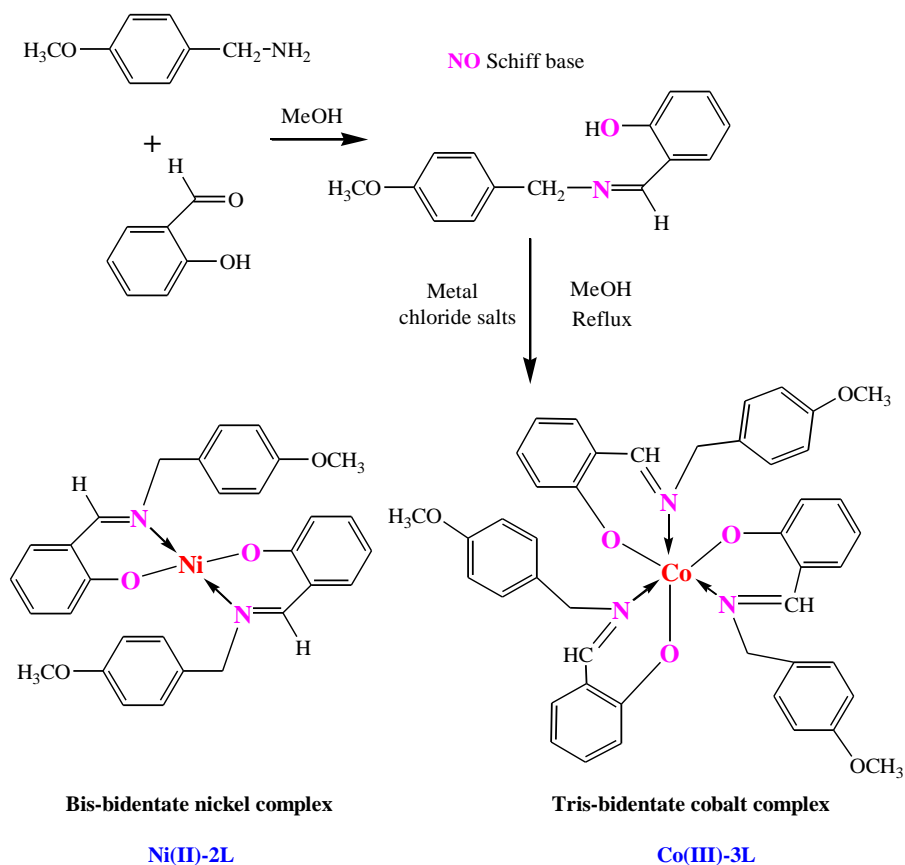
1. INTRODUCTION

Schiff bases are the condensation product of primary amine and aldehyde or ketone that are employed as ligands in coordination chemistry with several transition metals ion [1-6]. The structure of these metal Schiff base complexes can be tailored by wisely choosing the starting materials, what in

turn allows to selectively modify their properties and therefore their potential applications [7-10]. Thus, these compounds have been used widely in electrocatalysis [11], organic synthesis [12], corrosion inhibitors [13] and many biological activities [14].

The number and the nature of the donor atoms of the Schiff base ligands make them very excellent candidates to synthesize metal complexes. Salicylaldehyde and its derivatives are especially useful among carbonyl precursors for the synthesis of a large variety of Schiff bases, what can be achieved by reacting them with different kinds of primary amines. Such condensation reactions lead to bidentate ligands containing imine groups, which can be used as the modulators of structural and electronic properties of transition metal centers [15,16].

The catalytic reduction of alkyl and aryl halides by transition metal Schiff base complexes is subject of growing interest in past few decades. On the other hand, considerable research has been focused to the electrochemical behavior of nickel and cobalt complexes in different solvents. Part of this research is devoted to the development of effective reduction electrocatalysis [17-20]. In this sense, the cobalt complexes were used as homogeneous catalysts for reductive cleavage of halogenated organic compounds such as, bromoethane [21], 1-bromobutane [22], bromobenzene [21], 1-iodobutane [23], 1-iododecane [24], benzyl chloride [25], 1,8-diiodooctane [26] and 2,6-bis(chloromethyl)pyridine [27]. The cobalt(I) electrogenerated react with alkyl or aryl halides to form an organocobalt(III) intermediate, followed by further reduction of the latter to get the desirable products. As for nickel complexes, they have been also employed for the catalytic cleavage of carbon-halogen bonds in a variety of organic compounds [28-30].



Scheme 1 Preparation procedure of HL and its metal complexes of Ni(II)-2L and Co(III)-3L.

Keeping in view the huge interest in the synthesis of new catalysts agents and according to the appropriate electrochemical performance previously mentioned for cobalt and nickel Schiff base complexes, we describe herein the synthesis of mononuclear complexes of Co(III) and Ni(II) containing bidentate Schiff base ligand obtained from condensation of 4-methoxybenzylamine and salicylaldehyde (Scheme 1). Both complexes have been characterized by different analytical and spectroscopic methods. Cyclic voltammetry has been carried out in order to investigate the electrochemical behavior of nickel and cobalt complexes as well as their catalytic efficiency towards the electroreduction of bromocyclopentane.

2. EXPERIMENTAL

2.1. Reagents and instrument

The following chemicals were commercial products purchased from Sigma-Aldrich: Salicylaldehyde, 4-Methoxybenzylamine, $\text{NiCl}_2 \cdot 6\text{H}_2\text{O}$, $\text{CoCl}_2 \cdot 6\text{H}_2\text{O}$, Tetra-*n*-ethylammonium tetrafluoroborate, bromocyclopentane, iodobenzene, methanol and dimethylformamid. All these reagents and solvents were used as received without further purification.

Purity of the synthesized Schiff base HL and their complexes was checked by TLC. The melting points were measured on a Kofler Bank 7779 apparatus. Chemical analysis of C, H and N was performed using a LECO TruSpec Micro CHNS elemental micro analyzer. FT-IR spectra were recorded on Perkin-Elmer 1000 spectrophotometer, with sample being diluted in KBr pellets ($4000\text{--}400\text{ cm}^{-1}$) while the electronic spectra were obtained on a Unicam UV-300 Spectrophotometer with DMF solutions (1 cm, cell) in the 200-800 nm range. ^1H NMR and ^{13}C NMR spectra were recorded on a Bruker 400 MHz spectrometer with CDCl_3 as solvent and tetramethylsilane (TMS) as the internal standard. Chemical shifts (δ) are expressed in ppm.

Electrochemical measurements were performed using a potentiostat Voltalab 40 model PGZ 301. The cyclic voltammograms were carried out in cell of 5 ml provided with three-electrode under an inert atmosphere at room temperature, consisting of a glassy carbon (GC) as working electrode (diameter 3 mm) and a platinum wire as the counter electrode (CE). All the potentials are quoted versus the saturated calomel electrode (SCE). The glassy carbon working electrode was manually cleaned with diamond paste and rinsed with acetone and DMF polish prior to each scan. The supporting electrolyte was 0.1 M Tetra-*n*-ethylammonium tetrafluoroborate (Et_4NBF_4) in DMF as solvent.

2.2.1. Preparation of the ligand HL

The Schiff base ligand, 2-[(4-Methoxybenzyl)iminomethyl]phenol HL, was synthesized from a methanolic solution (6 ml) of salicylaldehyde (122 mg, 1 mmol) and a methanolic solution (6 ml) of 4-Methoxybenzylamine (137.18 mg, 1 mmol) [31]. The mixed solution instantly turned yellow and was then stirred under reflux for 2 hours. Yellow crystals were produced by slow evaporation of ligand

solution at room temperature for 7 days. Yield: 71%, m.p. 80°C. Microanalysis of $C_{15}H_{15}NO_2$ found (calc.) was: C 75.18 % (74.67); H 6.16 % (6.27); N 5.95 % (5.81).

2.2.2. Preparation of the Complex Ni(II)-2L

The nickel complex Ni(II)-2L was obtained from warm methanolic solution of the Schiff base HL (1 mmol) to which a solution of $NiCl_2 \cdot 6H_2O$ (118.83 mg, 0.5 mmol) in methanol (5 ml) was dropwisely added [32]. This mixture was stirred and boiled under reflux for 4 hours. The product was precipitated as a green powder. The precipitate was then filtered off, washed with cold methanol, dried and stored. Yield: 43%, m.p. 198°C. Microanalysis of $C_{30}H_{28}N_2O_4Ni$ found (calc.) was: C 67.59 % (66.82); H 5.14 % (5.23); N 5.13 % (5.19).

2.2.3. Preparation of the Complex Co(III)-3L

This complex was prepared by using the following procedure: A solution of $CoCl_2 \cdot 6H_2O$ (80.92 mg, 0.34 mmol) in methanol (5 ml) was added dropwise to a warm solution of the Schiff base HL (1 mmol). This mixture was stirred and maintained under reflux for about 3 hours. The product was precipitated as a green powder. The precipitate was then filtered off, washed with cold methanol. Dark green single crystals of Co(III)-3L suitable for X-ray analysis were obtained by slow evaporation of the filtrate. Yield: 33%, m.p. 228°C. Microanalysis of $C_{45}H_{42}N_3O_6Co$ found (calc.) was: C 69.42 % (69.31); H 5.33 % (5.43); N 5.46 % (5.39).

3. RESULTS AND DISCUSSION

3.1. Chemistry

The present study is based upon the employment of bidentate Schiff-base ligand (HL), which is obtained by reacting 4-methoxybenzylamine and salicylaldehyde in 1:1 molar ratio. The corresponding complexes were synthesized by the reactions of HL with chloride metal salts ($NiCl_2 \cdot 6H_2O$ and $CoCl_2 \cdot 6H_2O$) in methanol to obtain Ni(II)-2L and Co(III)-3L, respectively. All synthesized compounds were stable at room temperature and soluble in common organic solvents such as CH_2Cl_2 , ACN, DMF and DMSO.

3.2. Spectroscopic properties

➤ Electronic spectra

UV-Vis absorption spectra of HL and the two complexes in DMF solutions have been studied in the range of 290-700 nm, as illustrated in Fig. 1. The ligand HL shows only intense absorption band at 316 nm, assigned to the $n-\pi^*$ transition of azomethine chromophore [33,34]. This band is shifted to

the 325 nm in the spectrum of the nickel complex showing a bathochromic effect, confirming the presence of azomethine–metal coordination as expected [35]. However, this last band is absent in the spectrum of the cobalt complex [36]. The other broad band appears at around 400 nm, which is attributed to charge transfer transition of the Co(III)-3L complex [37]. The d-d transitions appear in the range 500–700 nm in the cobalt(III) and nickel(II) complexes. The Ni(II)-2L complex has a single d-d band at 614 nm, consistent with square planar stereochemistry [38]. The Co(III)-3L complex has two d-d bands at 588 and 653 nm. These electronic transitions are characteristic of a cobalt(III) complex in a six-coordinate octahedral geometry [39].

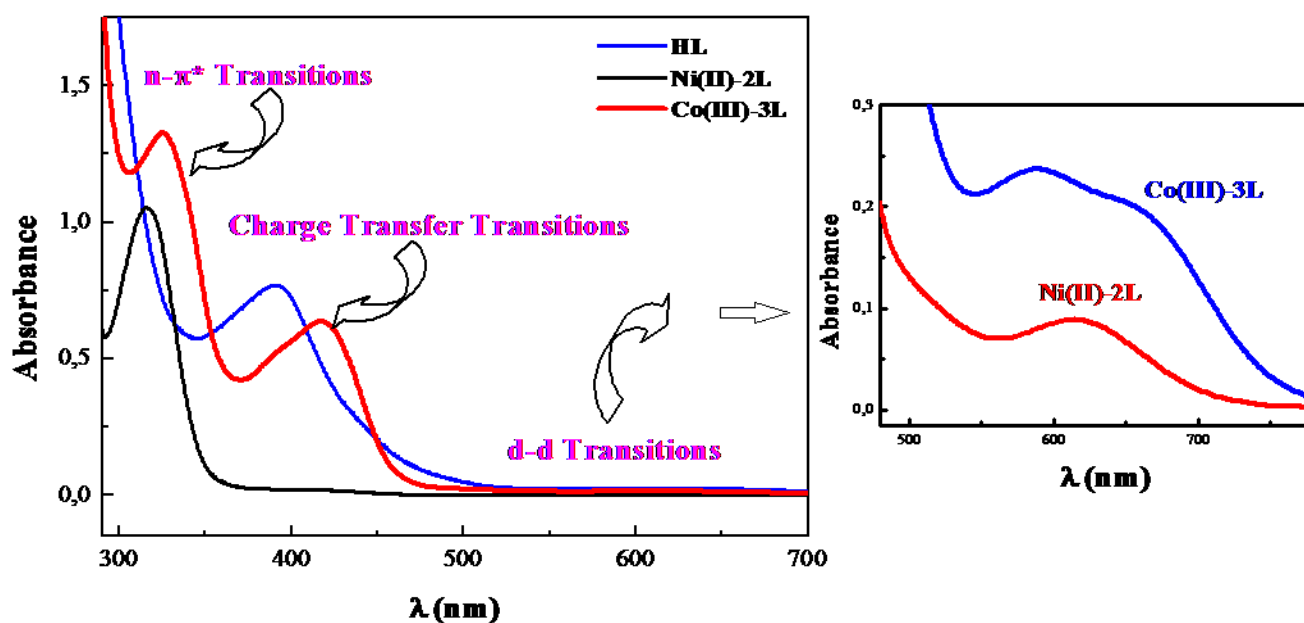


Figure 1. UV–Vis spectra of ligand **HL** and its metal complexes **Ni(II)-2L** and **Co(III)-3L** in DMF, the inset shows d–d transition region of the two complexes.

➤ Infrared spectra

FT-IR spectroscopy is a useful technique for determining the functionalities on the novel synthesized compounds. The FT-IR spectrum of HL ligand has been compared with that of the Ni(II)-2L and Co(III)-3L complexes in order to confirm the coordination of HL to the metals ions, in the region 4000–400 cm^{-1} . The FT-IR spectra of ligand and its nickel and cobalt complexes are found to be quite complex, exhibiting a large number of bands with varying intensities. Accordingly, instead of showing the full spectra, the most important stretching frequencies of the FT-IR spectral features of the two complexes and free ligand have been shown in Table 1.

The FT-IR spectrum of the free ligand HL presents a broad band characteristic of the OH group centered at 3448 cm^{-1} . The strong band observed at 1624 cm^{-1} is due to azomethine (C=N) stretching vibration [3]. This band is shifted to the 1606 cm^{-1} in Co(III)-3L and 1612 cm^{-1} in Ni(II)-2L, indicating the participation of azomethine nitrogen in coordination [40,24]. The band located at 1454 cm^{-1} and 1253 cm^{-1} can be attributed to the C–N and C–O stretching of the of the ligand. But after complexation

of C–N and C–O group via nitrogen and oxygen to the metal ion, these bands were shifted to 1391 and 1324 cm^{-1} [41] for Ni(II)-2L, and to 1387 and 1320 cm^{-1} for Co(III)-3L [42]. Finally, the FT-IR spectra of the both complexes show new bands in the regions 590-591 and 436-469 cm^{-1} . These bands can be assigned to $\nu(\text{M-O})$ and $\nu(\text{M-N})$ stretching vibrations, respectively [43,44].

Table 1. FT-IR (ν/cm^{-1}) spectral data for **HL** and its metal complexes.

Compound	$\nu(\text{OH})$ (Broad)	$\nu(\text{C=N})$	$\nu(\text{C=C})$	$\nu(\text{C-N})$	$\nu(\text{C-O})$	$\nu(\text{M-N})$	$\nu(\text{M-O})$
HL	3448	1624	1505	1378	1314	–	–
Ni(II)-2L	–	1606	1509	1391	1324	436	591
Co(III)-3L	–	1612	1515	1387	1320	469	590

3.1.3. ^1H and ^{13}C NMR spectra

The ^1H and ^{13}C NMR spectra of the ligand HL and its diamagnetic nickel and cobalt complexes were recorded in CDCl_3 solutions and chemical shifts are reported in Tables 2 and 3. In the ^1H NMR spectrum of the Schiff base HL (Fig. 2), the phenolic OH proton appears as a broad singlet in the offset region at 13.494 ppm [45]. The characteristic signal at 8.431 ppm, is due to the azomethine ($-\text{HC=N}$) proton [46]. In the aromatic region, multiplets are observed between 7.356 and 6.884 ppm [47], which can be attributed to protons of benzene rings of the ligand. Two signals appearing at 4.773 and 3.830 ppm can also be assigned to methylene (N-CH_2) protons and methoxy (O-CH_3) protons, respectively [48].

In addition to this, the disappearance of signal of the hydroxyl protons in the spectra of complexes indicates that the OH groups become deprotonated after coordination. A downward shift (7.428 ppm) of the azomethine protons (HC=N) signal with respect to the corresponding free ligand is observed for Co(III)-3L; the same signal is also shifted in the spectrum of the nickel complex Ni(II)-2L to 10.405 ppm, suggesting the involvement of azomethine nitrogen in the coordination with metal ion [43,49]. In the case of the latter, the three (HC=N) protons give only one signal, which is slightly broader than that of the free ligand, suggesting a composite nature [50]. The aromatic protons of the three aromatic benzene rings in the coordinated Schiff base ligand appear in the appropriate region. The aliphatic protons (N-CH_2 and OCH_3) for the Co(III)-3L complex have been detected in the range of 4.055 to 4.878 and 3.805 to 3.830 ppm respectively. As for Ni(II)-2L, they have been obtained at 5.457 and 3.845 ppm respectively.

^{13}C NMR spectral data were consistent with ^1H NMR spectral data. For Schiff base ligand HL, the peak appearing at 165.193 ppm is assignable to the imine carbon atoms [9]. On the other hand, the resonance signals observed in the region 132.311 to 114.082 ppm is attributed to phenyl function of the ligand. The aliphatic N-CH_2 and OCH_3 carbon peaks of the ligand are detected at 62.568 and 55.344 ppm, respectively (See Fig. 2). The same signals are present in the ^{13}C NMR spectra of the

Ni(II)-2L and Co(III)-3L complexes but, they have shifted downfield invoking coordination of the ligand to Co(III) or Ni(II) ions through its azomethine groups. The observed three-line pattern in the ^{13}C NMR spectrum of Co(III)-3L is indicative of a tris-chelate structure [51]. These chemical shifts may be approached to those reported in the literature [52,43].

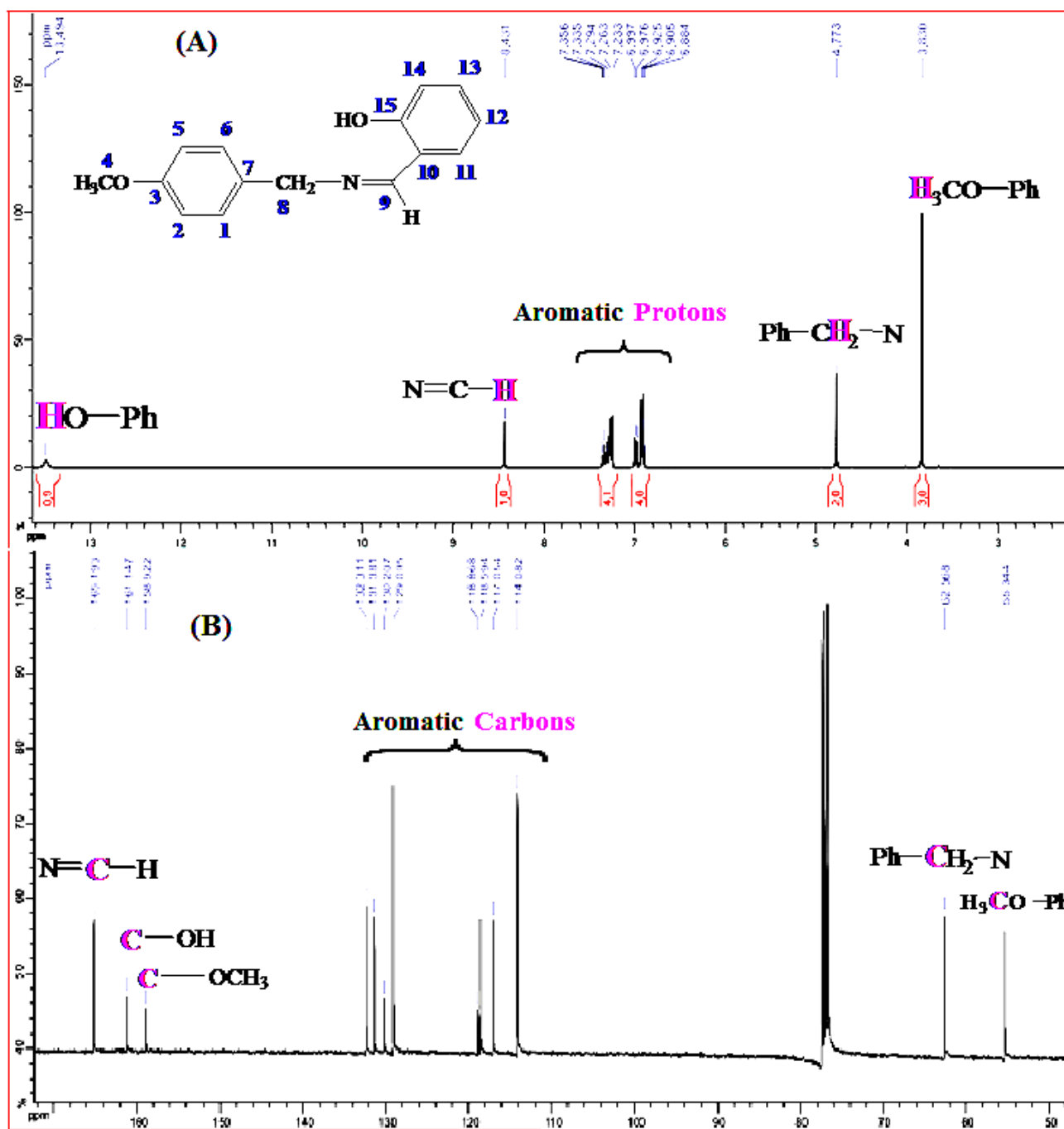


Figure 2. (A) ^1H NMR and (B) ^{13}C NMR spectra of the Schiff base HL.

Table 2. ^1H NMR and ^{13}C NMR spectral data of the Schiff base HL and its metal complexes Ni(II)-2L and Co(III)-3L (in CDCl_3); δ in ppm; s, singlet; dd, doublet of doublets; m, multiplet.

^1H NMR	OH	$\text{N}=\text{CH}_{(9)}$	$\text{H}_{(1-2, 5-6, 11-14)}$	$\text{N}-\text{CH}_2(8)$	$\text{OCH}_3(4)$
^{13}C NMR	-	$\text{N}=\text{C}_{(9)}\text{H}$	$\text{C}_{(1-3, 5-7, 10-15)}$	$\text{N}-\text{CH}_2(8)$	$\text{OCH}_3(4)$
HL	13.487(s, 1H)	8.432 (s, 1H)	6.888-7.301(m, 8H)	4.775(s, 2H)	3.833(s, 3H)
	-	165.194	100 to 140	62.577	55.358
Ni(II)-2L	-	10.405(s, 1H)	6.319-7.521(m, 8H)	5.457(s, 2H)	3.845(s, 3H)
	-	164.751	114.075to 133.309	60.366	55.313
Co(III)-3L	-	7.428(s, 3H)	6.455-7.138(m, 24H)	4.055-4.88 (dd, 6H)	3.816(s, 9H)
	-	165.888		60.562	55.327
	-	165.888	113.848to134.138	60.205	55.327
		165.888		59.924	55.356

3.2. Electrochemical characterization

The electrochemical behavior of HL ligand and corresponding complexes Ni(II)-2L and Co(III)-3L were studied at room temperature by cyclic voltammetry in DMF solution containing 0.1 M Et_4NBF_4 at scan rate of $100 \text{ mV}\cdot\text{s}^{-1}$ over a potential range from -2.2 to +1.5 V. vs. SCE, Fig. 3. An oxidation wave can be observed at $E_{p_a} = 1.21 \text{ V. vs. SCE}$ in the CV that may be assigned to the oxidation of the phenolic group, as reported in the literature [53]. During the reduction sweep, HL presents a peak at $E_{p_c} = -1.89 \text{ V. vs. SCE}$, due to the reduction imino group [54]. Cyclic voltammetry of the complexes Ni(II)-2L and Co(III)-3L was performed in potential ranges of -2.2 to 1.5 V. vs. SCE and -1.6 to 0.8 V. vs. SCE, respectively. The cyclic voltammogram of Ni(II)-2L (Fig. 3) shows a well-defined oxidation peak at $E_{p_{a1}} = -1.46$, followed by three oxidation waves at $E_{p_{a2}} = 0.8 \text{ V. vs. SCE}$, $E_{p_{a3}} = 0.97 \text{ V. vs. SCE}$ and $E_{p_{a4}} = 1.20 \text{ V. vs. SCE}$ in the anodic scan. The first and the second ones are assigned to the Ni(I)/Ni(II) and Ni(II)/Ni(III) oxidation reactions, while the last two oxidative processes can be attributed to the oxidation of the bidentate Schiff base. In the reverse scan, two clear cathodic peaks are obtained at $E_{p_{c1}} = 0.63$ and $E_{p_{c2}} = -1.56 \text{ V. vs. SCE}$. The former one corresponds to the reduction of Ni(III)/Ni(II) couple, whereas the latter one to Ni(II)/Ni(I) couple [55].

In the case of Co(III)-3L complex, the cyclic voltammogram exhibits two systems redox which are attributed to Co(II)/Co(I) ($E_{1/2} = -0.92 \text{ V. vs. SCE}$) and Co(III)/Co(II) ($E_{1/2} = 0.01 \text{ V. vs. SCE}$) redox processes, respectively. The first couple shows an anodic peak at $E_{p_{a1}} = -0.78 \text{ V. vs. SCE}$ with its corresponding cathodic peak at -1.06 V. vs. SCE [37], and the peak to peak separation (ΔE_p) is evaluated to 0.29 V. Whereas the second couple [Co(II)/Co(I)] is observed with a cathodic peak potential $E_{p_c} = -0.33 \text{ V. vs. SCE}$, an anodic peak potential $E_{p_a} = 0.32 \text{ V. vs. SCE}$ [56], and also the peak to peak separation (ΔE_p) is equal to 0.65 V. These results suggest that the first couple behaved as a quasi-reversible redox process while the second as an irreversible redox system. These redox systems of Co(III)-3L are both proposed as monoelectronic transfers.

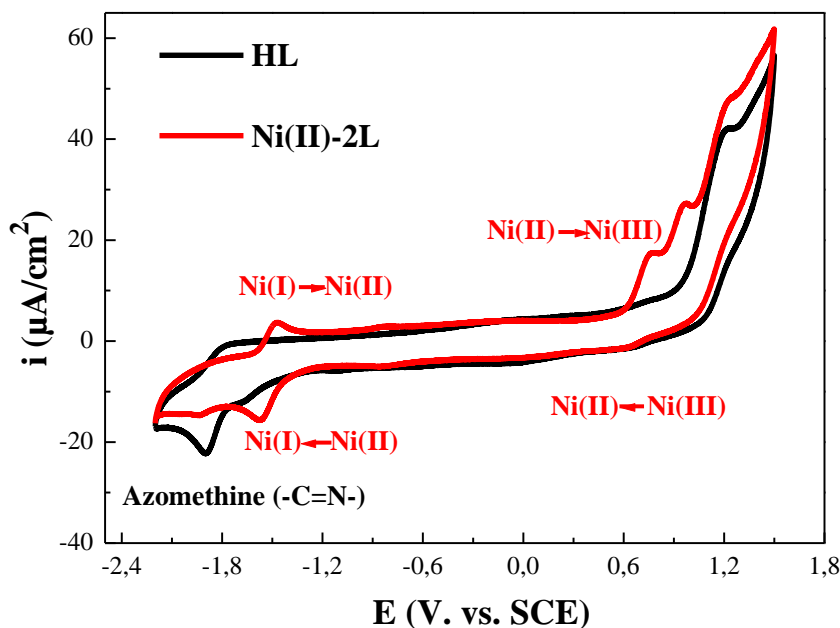


Figure 3. Cyclic voltammogram of 1 mM solution of HL (—) and Ni(II)-2L (—) in DMF containing 0.1 M Et₄NBF₄ at scan rate 100 mV.s⁻¹.

➤ *Effect of scan rates*

We have checked the effect of scan rate for the Ni(II)/Ni(I) redox process by cycling in the potential range to -1.2-1.8 V. vs. SCE (Fig. 4) on glassy carbon electrode in the same electrochemical system previously reported in Fig. 3. The initial CV, Fig. 4A, shows a well-defined redox peak at $E_{pa} = -1.47$ V. vs. SCE (anodic peak) and $E_{pc} = -1.57$ V. vs. SCE (cathodic peak) corresponding to Ni(II)/Ni(I) system. The peak to peak separation between the anodic and cathodic potentials at this scan rate is $\Delta E_{p1} = 100$ mV. The current intensity and the evolution of the peak position of this redox system has been tracked at different scan rates between 10 and 500 mV.s⁻¹, the results obtained being illustrated in Fig. 4B. A continuous increasing of both anodic and cathodic peak currents (i_{pa} , i_{pc}) accompanied with a neat shifting of the anodic and cathodic potentials to the positive and negative values, respectively. The linear dependency of both anodic and cathodic peak currents (i_{pa} , i_{pc}) with the square root of the scan rate ($v^{1/2}$) was noted (Fig. 4 curve C). This behavior was attributed to an electrochemical process, mainly diffusion-controlled. Furthermore, the anodic and cathodic peak potentials (E_{pa} , E_{pc}) are proportional to the logarithm of the scan rate (Log v) as below demonstrated (See Fig. 4 curve D).

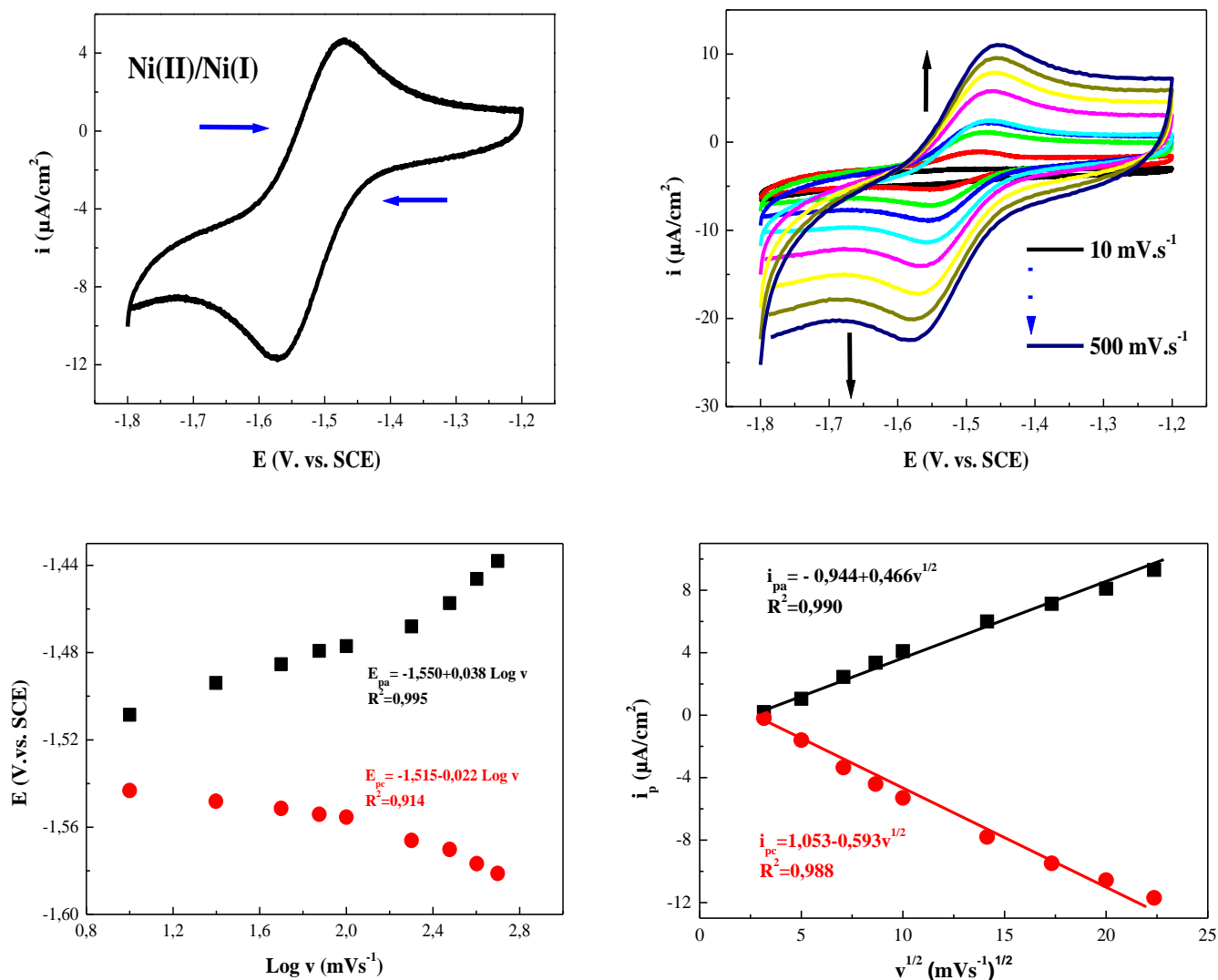


Figure 4. (A) Cyclic voltammograms of nickel complex recorded in the range between -1.2 and -1.8 V. vs. SCE using $100 \text{ mV}\cdot\text{s}^{-1}$ as scan rate; (B) Same experimental conditions with various scan rates (10, 25, 50, 75, 100, 200, 300, 400 and $500 \text{ mV}\cdot\text{s}^{-1}$); (C) Anodic and cathodic potentials (E_{pa}/E_{pc}) versus $\text{Log } v$; (D) Anodic and cathodic peak currents (I_{pa}/I_{pc}) versus square root of the scan rate ($v^{1/2}$).

3.3. Electrocatalysis

Lastly, we have analyzed the catalytic reduction of Bromocyclopentane by the synthesized Ni(II)-2L and Co(III)-3L complexes in 0.1 M $\text{Et}_4\text{NBF}_4/\text{DMF}$ solutions. Fig. 5 shows the CVs obtained at $100 \text{ mV}\cdot\text{s}^{-1}$ scan rate using a fixed Ni(II)-2L concentration of $1 \mu\text{M}$, while different concentrations of bromocyclopentane and iodobenzene (2, 3, 4 and $8 \mu\text{M}$) were tested in this electrocatalytic study. Curve A (black line) in both CVs shows the Ni(II)/Ni(I) redox couple as previously mentioned. After addition of $2 \mu\text{M}$ of either bromocyclopentane or iodobenzene (B curves in Fig. 5 A-B), the characteristic behavior of an electrochemical catalytic process is observed: the reduction current

increases progressively with a peak potential of -1.59 V whereas the anodic peak expressing the oxidation reaction of Ni(I) decreases rapidly. When the concentration is further increased for both aliphatic and aromatic halides (2, 3, 4 and 8 μM), the anodic peak describing the reoxidation of Ni(I) species disappears and the cathodic peak current grows consequently. However, this increasing is not in linear relationship towards the substrate concentration. This behavior indicates sluggish or incomplete regeneration of Ni(II)-2L specie [30,57].

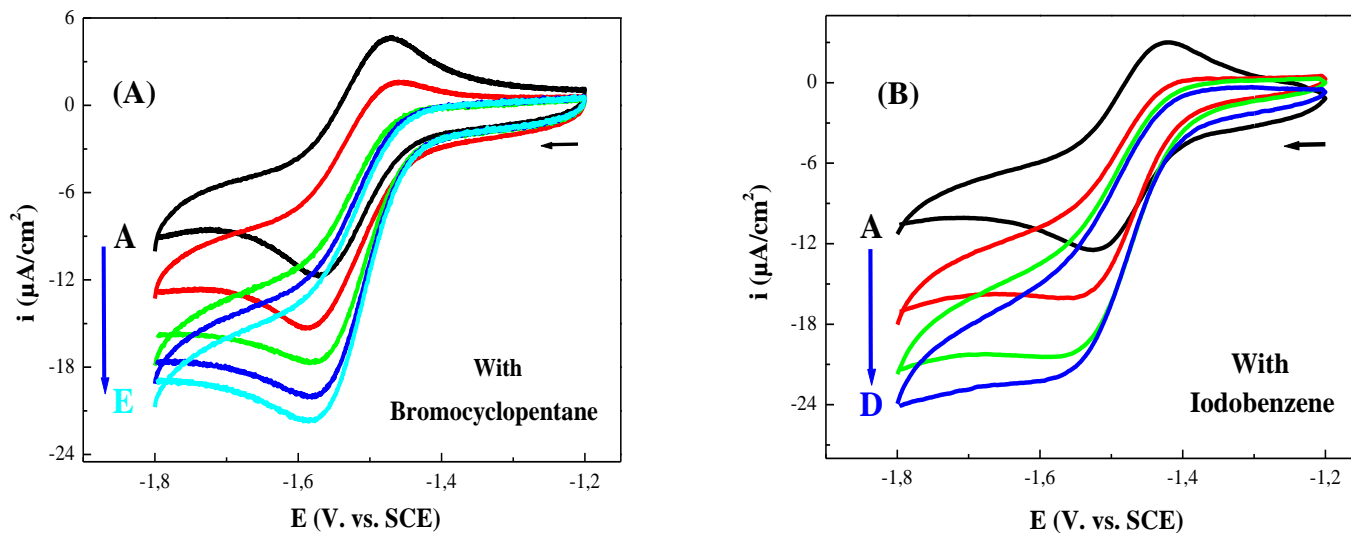


Figure 5. Cyclic voltammograms of the electrocatalytic reduction of **A)** bromocyclopentane and **B)** iodobenzene at different concentrations (DMF/ Et_4NBF_4 , 0.1 M) using a 1.0 mM solution of Ni(II)-2L complex as catalyst. Scan rate of $100 \text{ mV}\cdot\text{s}^{-1}$.

Furthermore, Fig. 6 shows the effect of different bromocyclopentane and iodobenzene concentrations on the electrochemical response of a 2 mM solution of Co(III)-3L complex recorded under similar experimental conditions (potential range of -1.6 - 0.3 V. vs. SCE). Again, the curve A depicts the initial Co(II)/Co(I) redox couple. In the presence of $1\mu\text{M}$ of each halide (curve B), important changes are observed. So, the cathodic current corresponding to the regeneration of Co(I) complex in the interface electrode-solution increases while the anodic current, due to the oxidation of Co(I) complex decreases. This decrease may be explained by the consumption of the cobalt species in the diffusion layer via reaction with bromocyclopentane and iodobenzene [58].

By increasing the concentration of (curves C, D, and E), a small peak appears at -0.84 V [59], the intensity of this new peak grows as the concentration of bromocyclopentane and iodobenzene increases. This peak is attributed to the formation of Co(I) species and its follow-up reaction with these halides intermediates leads to the formation an organocobalt(III) complex, which is further electroreduced [60]. The cathodic peak shifted to the negative potentials while the anodic peak was completely disappeared [24]. This is due to the fast catalytical reaction with the substrate [61]. These observations can be considered a signal of the electrocatalytic reduction by electrogenerated Co(II) species.

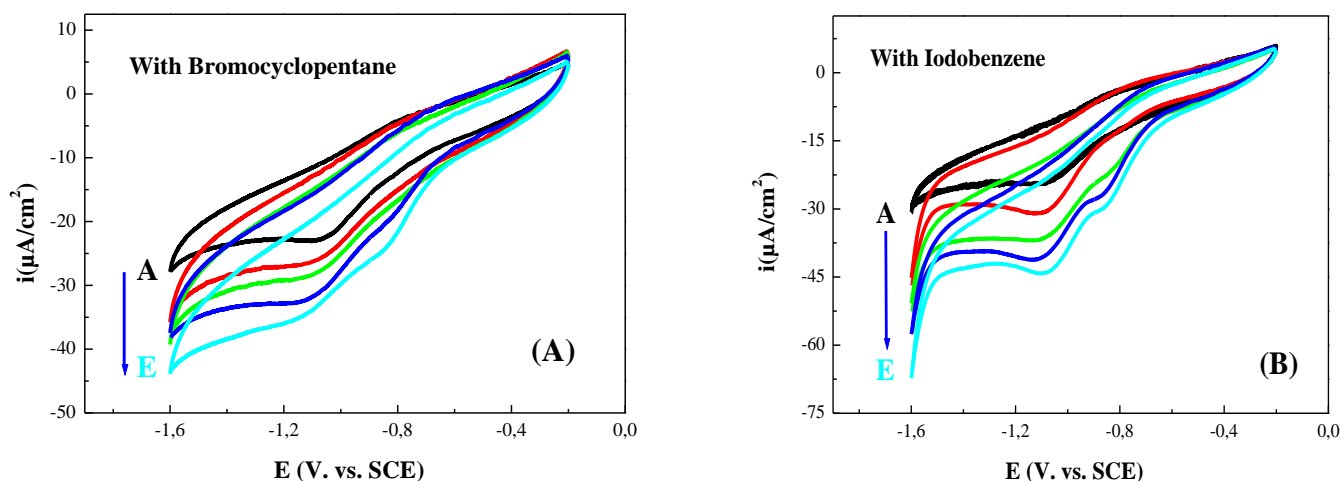


Figure 5. Cyclic voltammograms of the electrocatalytic reduction of (A) bromocyclopentane and (B) iodobenzene at different concentrations (DMF/Et₄NBF₄, 0.1 M) using a 2.0 mM solution of Co(III)-2L complex as catalyst and 100 mV.s⁻¹ as scan rate.

4. CONCLUSION

In conclusion, we have investigated the synthesis and characterization of asymmetric bidentate (ON) Schiff base ligand (HL) and its mononuclear nickel and cobalt Schiff base complexes, Ni(II)-2L and Co(III)-3L. NMR, electronic and FT-IR spectral analysis have been confirmed the tetra- (N₂O₂) and octa- (N₃O₃) coordinated forms of the both complexes. Moreover, the electrochemical behavior of the ligand and its metal complexes were studied by cyclic voltammetry. These voltammetric studies showed interesting redox systems. Accordingly, these complexes were used as homogeneous electrocatalysts in DMF solutions containing 0.10 M Et₄NBF₄ as supporting electrolyte and glassy carbon electrode for the reduction of two kinds of halides: bromocyclopentane and iodobenzene as aliphatic and aromatic substrates. These both complexes were found to be able to catalyze the reduction of the two halides. We also believe that this work will shed light on future works on the synthesis of numerous Schiff base–metal complexes using bi-, tri-, and tetradentate Schiff base ligands containing methoxy functional groups. Furthermore, it was envisaged that these compounds will be involved in the electrode modification for many applications, such as electrocatalysis, electroanalysis and as well in the detection of biomolecules.

ACKNOWLEDGMENTS

The authors would like to thank the MESRS and DG-RSDT (Ministère de l'Enseignement Supérieur et de la Recherche Scientifique et la Direction Générale de la Recherche - Algérie) for financial support. This work is supported by the Ministerio de Economía y Competitividad (MAT2016-76595-R).

References

1. J. Zhang, F. Pan, H. Cheng and W. Du, Synthesis, *Synth. React. Inorg. Met-Org. Nano-Met. Chem.*, 40 (2010) 211.
2. G. Grivani, V. Tahmasebi, K. Eskandari, A.D. Khalaji, G. Bruno and H.A. Rudbari, *J. Mol. Struct.*, 1054–1055 (2013) 100.
3. B. Shafaatian, A. Soleymannpour, N.K. Oskouei, B. Notash and S.A. Rezvani, *Spectrochim. Acta Part A*, 128 (2014) 363.
4. M. Köse, G. Ceyhan, M. Tümer, I. Demirtas, I. Gönül and V. McKee, *Spectrochim. Acta Part A*, 137 (2015) 477.
5. A. Jain, M. Gupta, A. Bhardwaj and T.R. Thapak, *Res. J. Chem. Sci.*, 5 (2015) 39.
6. S.M. Wilkinson, T.M. Sheedy and E.J. New, *J. Chem. Educ.*, 93 (2016) 351.
7. M. Odabaşoğlu, F. Arslan, H. Ölmez and O. Büyükgüngör, *Dyes. Pigm.*, 75 (2007) 507.
8. S. Mandal, A.K. Rout, G. Pilet and D. Bandyopadhyay, *Trans. Met. Chem.*, 34 (2009) 719.
9. C. Şenol, Z. Hayvali, H. Dal and T. Hökelek, *J. Mol. Struct.*, 997 (2011) 53.
10. A.D. Khalaji, M. Nikookar and D. Das, *J. Therm. Anal. Calorim.*, 115 (2014) 409.
11. (a) A. Adhikari, S. Radhakrishnan and R. Patil, *Synth. Met.*, 159 (2009) 1682; (b) A. Ourari, N. Hellal, N. Charef and D. Aggoun, *Electrochim. Acta*, 170 (2015) 311.
12. A.R. Silva, T. Mourão and J. Rocha, *Cata. Today*, 203 (2013) 81.
13. Z. Zhang, N. Tiana, L. Zhanga and L. Wu, *Corr. Scien.*, 98 (2015) 438.
14. Z.H. Chohan, S.H. Sumrra, M.H. Youssoufi and T.B. Hadda, *Eur. J. Med. Chem.*, 45 (2010) 2739.
15. M. Amirnasr, A.H. Mahmoudkhani, A. Gorji, S. Dehghanpour and H.R. Bijanzadeh, *Polyhedron*, 21 (2002) 2733.
16. A. Sharma and M. Shah, *J. Appl. Chem.*, 3 (2013) 62.
17. M. Salehi, M. Amirnasr and K. Mereiter, *J. Iran. Chem. Soc.*, 7 (2010) 740.
18. A.D. Khalaji, S.M. Rad, G. Grivani, M. Rezaei, K. Gotoh and H. Ishida, *Chin. J. Chem.*, 29 (2011) 1613.
19. T. Okada, K. Katou, T. Hirose, M. Yuasa and I. Sekine, *J. Electrochem. Soc.*, 146 (1999) 2562.
20. A.H. Kianfar and S. Zargari, *J. Coord. Chem.*, 61 (2008) 341.
21. G. Costa, A. Puxeddu and E. Reisenhofer, *J. Chem. Soc. Dalton Trans.*, (1973) 2034.
22. D. Pletcher and H. Thompson, *J. Chem. Soc. Faraday Trans.*, 93 (1997) 3669.
23. D. Pletcher and H. Thompson, *J. Electroanal. Chem.*, 464 (1999) 168.
24. A. Ourari, S. Messali, B. Bouzerafa, Y. Ouennoughi, D. Aggoun, M.S. Mubarak, L.M. Strawsine and D.G. Peters, *Polyhedron*, 97 (2015) 197.
25. A.A. Isse, A. Gennaro and E. Vianello, *J. Electroanal. Chem.*, 444 (1998) 241.
26. K.S. Alleman and D.G. Peters, *J. Electroanal. Chem.*, 460 (1999) 207.
27. C. Ji, D.G. Peters, J.A. Karty, J.P. Reilly and M.S. Mubarak, *J. Electroanal. Chem.*, 516 (2001) 50.
28. C.E. Dahm and D.G. Peters, *J. Electroanal. Chem.*, 406 (1996) 119.
29. P.W. Raess, M.S. Mubarak, M.A. Ischay, M.P. Foley, T.B. Jennermann, K. Raghavachari and D.G. Peters, *J. Electroanal. Chem.*, 603 (2007) 124.
30. A. Ourari, Y. Ouennoughi, D. Aggoun, M.S. Mubarak, E.M. Pasciak and D.G. Peters, *Polyhedron*, 67 (2014) 59.
31. C. Phurat, T. Theerawattananond and N. Muangsin, *Acta Cryst.*, E66 (2010) o3298.
32. H. Bahron, A.M. Tajuddin, W.N.W. Ibrahim, H.K. Func and S. Chantrapromma, *Acta Cryst.*, E70 (2014) 104.
33. Y. Song, Z. Xu, Q. Sun, B. Su, Q. Gao, H. Liu and J. Zhao, *J. Coord. Chem.*, 61 (2008) 1212.
34. M. Salehi, M. Amirnasr, S. Meghdadi, K. Mereiter, H.R. Bijanzadeh and A. Khaleghian, *Polyhedron*, 81 (2014) 90.
35. A. Ourari, C. Zoubeydi, W. Derafa, S. Bouacida, H. Merazig and E. Morallon, *Res. Chem. Intermed.*, 43 (2017) 3163.

36. H. Iranmanesh, M. Behzad, G. Bruno, H.A. Rudbari, H. Nazari, A. Mohammadi and O. Taheri, *Inorg. Chim. Acta*, 395 (2013) 81.
37. F. Fadaee, M. Amirnasr and K. Schenk-Joß, *J. Iran. Chem. Soc.*, 10 (2013) 1067.
38. A.D. Khalaji, G. Grivani, M. Rezaei, K. Fejfarova and M. Dusek, *Polyhedron*, 30 (2011) 2790.
39. L.Q. Chai, J.J. Huang, H.S. Zhang, Y.L. Zhang, J.Y. Zhang and Y.X. Li, *Spectrochim. Acta Part A*, 131 (2014) 526.
40. A. Ghaffari, M. Behzad, M. Pooyan, H.A. Rudbari and G. Bruno, *J. Mol. Struct.*, 1063 (2013) 1.
41. B. Bouzerafa, A. Ourari, D. Aggoun, R. Ruiz-Rosas, Y. Ouennoughi and E. Morallon, *Res. Chem. Intermed.*, 42 (2016) 4839.
42. M. Dolaz and M. Tümer, *Trans. Met. Chem.*, 29 (2004) 516.
43. A. Ourari, I. Bougossa, S. Bouacida, D. Aggoun, R. Ruiz-Rosas, E. Morallon and H. Merazig, *J. Iran. Chem. Soc.*, 14 (2017) 703.
44. S. Menati, H.A. Rudbari, M. Khorshidifard and F. Jalilian, *J. Mol. Struct.*, 1103 (2016) 94.
45. Y.W. Dong, R.Q. Fan, P. Wang, L.G. Wei, X.M. Wang, H.J. Zhang, S. Gao, Y.L. Yang and Y.L. Wang, *Dalton Trans.*, 44 (2015) 5306.
46. C. Demetgül, M. Karakaplan, S. Serin and M. Diğrak, *J. Coord. Chem.*, 62 (2009) 3544.
47. C. Demetgül, D. Deletioğlu, F. Karaca, S. Yalçinkaya, M. Timur and S. Serin, *J. Coord. Chem.*, 63 (2010) 2181.
48. R. Vafazadeh and M. Kashfi, *Bull. Kor. Chem. Soc.*, 28 (2007) 1227.
49. A. Chakravorty and R.H. Holm, *Inorg. Chem.*, 3 (1964) 1521.
50. M. Shebl, S.M.E. Khalil, S.A. Ahmed and H.A.A. Medien, *J. Mol. Struct.*, 980 (2010) 39.
51. S.A. Samath, N. Raman, K. Jeyasubramanian and S.K. Ramalingam, *Polyhedron*, 10 (1991) 1687.
52. C.S.B. Gomes, S.A. Carabineiro, P.T. Gomes, M. Teresa Duarte and M.A.N.D.A. Lemos, *Inorg. Chim. Acta*, 367 (2011) 151.
53. P. Gili, M.G.M. Reyes, P.M. Zarza, I.L.F. Machado, M.F.C. Guedes da Silva, M.A.N.D.A. Lemos and A.J.L. Pombeiro, *Inorg. Chim. Acta*, 244 (1996) 25.
54. A.A. Isse, A. Cennaro and E. Vianello, *Electrochim. Acta*, 42 (1997) 2065.
55. A. Ourari and D. Aggoun, *J. Iran. Chem. Soc.*, 12 (2015) 1893.
56. E. López-Torres and M.A. Mendiola, *Polyhedron*, 24 (2005) 1435.
57. P. Vanalabhatana, D.G. Peters and J.A. Karty, *J. Electroanal. Chem.*, 580 (2005) 300.
58. E.R. Wagoner, C.P. Baumberger, A.A. Peverly and D.G. Peters, *J. Electroanal. Chem.*, 713 (2014) 136.
59. L.J. Klein, K.S. Alleman, D.G. Peters, J.A. Karty and J.P. Reilly, *J. Electroanal. Chem.*, 481 (2000) 24.
60. C. Ji, D.G. Peters, J.A. Karty, J.P. Reilly and M.S. Mubarak, *J. Electroanal. Chem.*, 516 (2001) 50.
61. C. Ji, S.E. Day and W.C. Silvers, *J. Electroanal. Chem.*, 622 (2008) 15.